Title	Magnetic Phases in Sr(1-x) Ca(x)Co(2)P(2) Studied by μ + SR
Author(s)	Sugiyama, Jun; Nozaki, Hiroshi; Harada, Masashi; Umegaki, Izumi; Higuchi, Yuki; Miwa, Kazutoshi; Imai, Masaki; Michioka, Chishiro; Yoshimura, Kazuyoshi; Ansaldo, Eduardo J.; Brewer, Jess H.; Andreica, Daniel; Baines, Christopher; Mansson, Martin
Citation	Physics Procedia (2015), 75: 426-434
Issue Date	2015
URL	http://hdl.handle.net/2433/226433
Right	© The Authors. Published by Elsevier B.V. This is an open access article under the CC BY-NC-ND license(https://creativecommons.org/licenses/by-nc-nd/4.0/)
Type	Journal Article
Textversion	publisher

Physics Procedia

Volume 75, 2015, Pages 426–434

20th International Conference on Magnetism

Magnetic phases in $Sr_{1-x}Ca_xCo_2P_2$ studied by μ^+SR

Jun Sugiyama[1,2*], Hiroshi Nozaki[1], Masashi Harada[1], Izumi Umegaki[1], Yuki Higuchi[1], Kazutoshi Miwa[1], Masaki Imai[3], Chishiro Michioka[3], Kazuyoshi Yoshimura[3], Eduardo J. Ansaldo[4], Jess H. Brewer[5,6], Daniel Andreica[7], Christopher Baines[8], and Martin Månsson[9]

[1] Toyota Central Research and Development Laboratories, Inc., Nagakute, Aichi, Japan
[2] Advanced Science Research Center, Japan Atomic Energy Agency, Tokai, Ibaraki, Japan
[3] Kyoto University, Kyoto, Japan
[4] University of Saskatchewan, Saskatoon, SK, Canada
[5] University of British Columbia, Vancouver, BC, Canada
[6] TRIUMF, Vancouver, BC, Canada
[7] Babes-Bolyai University, Cluj-Napoca, Romania
[8] Paul Scherrer Institut, Villigen PSI, Switzerland
[9] KTH Royal Institute of Technology, Stockholm, Sweden

Abstract

In order to elucidate the dependence of the magnetic ground state on the Ca content (x) in $Sr_{1-x}Ca_xCo_2P_2$ ($0 \leq x \leq 1$, $ThCr_2Si_2$-type structure), we have performed muon spin rotation and relaxation (μ^+SR) experiments on $Sr_{1-x}Ca_xCo_2P_2$ powder samples mainly in a zero applied field. The end member compound, $SrCo_2P_2$, is found to be paramagnetic down to 19 mK. As x increases, such a paramagnetic ground state is observed down to 1.8 K until $x = 0.45$. Then, as x increases further, a short-range antiferromagnetic (AF) ordered phase appears at low temperatures for $0.48 \leq x \leq 0.75$, and finally, a long-range AF ordered phase is stabilized for $x > 0.75$. The internal magnetic field of the other end member compound, $CaCo_2P_2$, is well consistent with that of the A-type AF order state, which was proposed from neutron scattering experiments. The phase diagram determined with μ^+SR is different from that proposed by macroscopic measurements. For an isostructural compound, $LaCo_2P_2$, static magnetic order is found to be formed below ~ 130 K.

Keywords: muon spin rotation and relaxation, cobalt phosphide, antiferromagnet, phase diagram

1 Introduction

Although iron pnictides with the $ThCr_2Si_2$-type (122) structure, e.g. $CaFe_2As_2$ and $BaFe_2As_2$, show unconventional superconductivity under pressure and/or with substitution for Ba by K

*email: e0589@mosk.tytlabs.co.jp

Selection and peer-review under responsibility of the Scientific Programme Committee of ICM 2015

doi:10.1016/j.phpro.2015.12.052

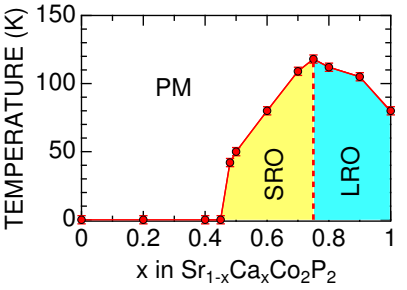

Figure 1: The variation of magnetic phases with x for $Sr_{1-x}Ca_xCo_2P_2$ determined with μ^+SR [8]. PM is a paramagnetic phase, SRO is a phase with wide field distribution probably due to short-range AF order, LRO is a long-range A-type AF ordered phase. Copyright 2015 American Physical Society.

[1, 2, 3], the related compounds AM_2P_2 with $A =$ Ca, Sr, or Ba, and $M =$ Fe, Co, or Ni exhibit, instead, interesting properties with associated structural changes. For the present target system, $Sr_{1-x}Ca_xCo_2P_2$, the crystal structure changes from an uncollapsed tetragonal (uc$T$) phase for $x = 0$ to a collapsed tetragonal (cT) phase for $x = 1$ [4]. Based on macroscopic measurements [4], the system evolves from a nonmagnetic metallic ground state to an AF metallic ground state through a crossover composition regime at $x \sim 0.5$. Then, in the x range between 0.8 and 0.9, the system manifests a ferromagnetic (FM)-like ground state within which the magnetic ordering temperature is highest for $x \sim 0.9$. For the sample with $x \geq 0.9$, an AF ground state reappears [5]. Similar behavior was also reported for $Ca(Fe_{1-x}Co_x)_2P_2$ [6], $Ca(Ni_{1-x}Co_x)_2P_2$ [6], and $SrCo_2(Ge_{1-x}P_x)_2$ [7].

However, according to our muon spin rotation and relaxation (μ^+SR) experiment on $Sr_{1-x}Ca_xCo_2P_2$ [8] (Fig. 1), a paramagnetic ground state is stable in the x range between 0 and 0.45 down to the lowest temperature measured. Then, as x increases from 0.45, a short-range antiferromagnetic (AF) ordered phase appears at low temperatures for $0.48 \leq x \leq 0.75$, and finally, a long-range AF ordered phase is stabilized for $x > 0.75$. The discrepancy between the phase diagram obtained by macroscopic measurements and that by μ^+SR is due to the unique spatial and time resolution of μ^+SR [9, 10, 11, 12, 13].

Since the phase diagram of $Sr_{1-x}Ca_xCo_2P_2$ was already described in detail [8], here, we report the detailed μ^+SR result on $SrCo_2P_2$, $CaCo_2P_2$ and an isostructural compound $LaCo_2P_2$.

2 Experimental

Polycrystalline samples of $SrCo_2P_2$, $CaCo_2P_2$, and $LaCo_2P_2$ were prepared from elemental P, Sr, Ca, La, and Co using a two step reaction. For the first step, SrP, CaP, LaP, and Co_2P were synthesized by a solid state reaction between Sr (Ca, La, Co) and P in an evacuated quartz tube at 800°C (700°C for Co_2P). In the second step, $SrCo_2P_2$, $CaCo_2P_2$, and $LaCo_2P_2$ were synthesized by a solid state reaction between SrP, CaP, LaP, and Co_2P at 1000°C for 20 hours in an Ar atmosphere. After grinding, the obtained powder was annealed two times at 1000°C for 40 hours in an Ar atmosphere [14].

High quality single-crystal platelets of $SrCo_2P_2$ were grown by a flux technique using ele-

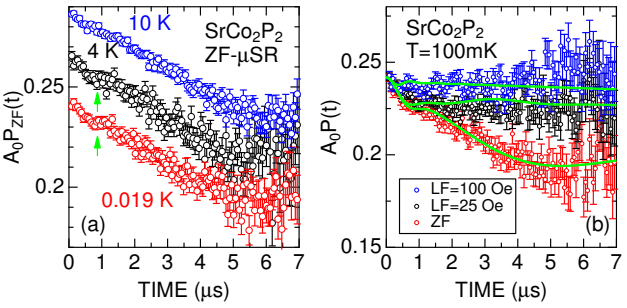

Figure 2: (a) The ZF-μ^+SR time spectrum for $SrCo_2P_2$ measured at 19 mK, 4 K, and 10 K. Green arrows represent the small minimum appeared at $T \leq 4$ K. Each spectrum is shifted upward by 0.02 for clarity of display. (b) The ZF- and two LF-μ^+SR spectra for $SrCo_2P_2$ measured at 100 mK. Solid lines in (b) represent the best fit with Eq. (1).

mental Sr, Co, and P as starting materials. Sn was used as the flux. The mixture of Sr, Co, P, and Sn were sealed in a quartz tube in an Ar atmosphere with 0.3 atm, and heated at 900°C for 72 hours, and then cooled down to 600°C with a rate of 3°C/h. The typical dimension of the crystal is $3 \times 3 \times 0.5$ mm^3.

According to powder x-ray diffraction (XRD) analyses, all the samples were almost single phase of tetragonal symmetry with space group $I4/mmm$. The μ^+SR spectra were measured at surface muon beam lines using the **LAMPF** spectrometer on M15 and M20 of TRIUMF in Canada and **Dolly** and **LTF** spectrometers of PSI in Switzerland. On **LAMPF** and **Dolly**, approximately 500 mg of powder sample was placed in an envelope with 1×1 cm^2 area, made of 0.05 mm thick Al-coated Mylar tape in order to minimize the background signal from the envelope. The envelope was attached to a low-background sample holder in a liquid-He flow-type cryostat for measurements in the T range between 1.8 and 150 K. At **LTF**, about 100 mg of platelets was attached onto a silver plate with an Apiezon-N grease, and the silver cell was set into a dilution refrigerator (DR) down to $T = 19$ mK. The experimental techniques are described in more detail elsewhere [9, 10].

3 Results and Discussion

3.1 $SrCo_2P_2$

Figure 2(a) shows the zero field (ZF-) μ^+SR spectra for the $SrCo_2P_2$ crystals recorded at $T = 19$ mK, 4 K and 10 K. The ZF-spectrum exhibits a clear Kubo-Toyabe type relaxation at 10 K, indicating a paramagnetic nature of $SrCo_2P_2$. However, a small minimum appears around $t = 1$ μs at 4 K and 19 mK, while the shape and position of the minimum does not depend on temperature at $T \leq 4$ K. Such behavior was also observed for a powder sample. In order to understand the nature of such minima, μ^+SR spectra were also recorded under ZF and in two longitudinal fields (LF = 25 and 100 Oe). (Here, a longitudinal field means the field parallel to the initial muon spin polarization.) Figure 2(b) shows the ZF- and two LF-μ^+SR spectra for the $SrCo_2P_2$ crystals obtained at 100 mK. The relaxation in the ZF-spectrum is clearly suppressed by LF, i.e. a decoupling behavior due to LF. The ZF- and LF-spectra

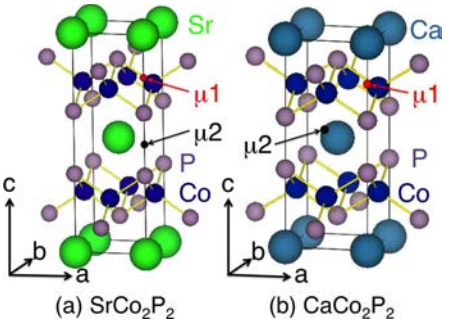

Figure 3: Muon sites in (a) $SrCo_2P_2$ and (b) $CaCo_2P_2$ deduced by DFT calculations [8]. The implanted muons are located at the 4*e* sites (μ_1 site) and 2*b* sites (μ_2 site) for $SrCo_2P_2$ and the 4*e* sites (μ_1 site) and 32*o* sites (μ_2 site) for $CaCo_2P_2$. The atomic position of each site is given in Table 1. Copyright 2015 American Physical Society.

were well fitted by a combination of two static Kubo-Toyabe functions $[G(\Delta, t, H_{\rm LF})]$ and a time-independent background signal from muons stopping in the silver plate.

$$A_0\, P(t) \quad = \quad A_{\rm KT1} G(\Delta_1, t, H_{\rm LF}) + A_{\rm KT2} G(\Delta_2, t, H_{\rm LF}) + A_{\rm BG}. \tag{1}$$

Here A_i are the asymmetries and Δ_i are the field distribution width at the muon sites. The fit for the ZF- and two LF-spectra using common $A_{\rm KT1}$, $A_{\rm KT2}$, $A_{\rm BG}$, Δ_1, and Δ_2 provided that $A_{\rm KT1} = 0.0144 \pm 0.0011$, $A_{\rm KT2} = 0.0364 \pm 0.0017$, $A_{\rm BG} = 0.1910 \pm 0.0018$, $\Delta_1 = (2.33 \pm 0.09) \times 10^6$ sec^{-1}, and $\Delta_2 = (0.337 \pm 0.014) \times 10^6$ sec^{-1}. This means that there are two different muon sites in the $SrCo_2P_2$ lattice, and the muons at the two sites sense a small random internal magnetic field. Therefore, $SrCo_2P_2$ is found to be a paramagnet even at 19 mK, being consistent with the recent study on a single crystal down to 1.5 K [15]. In addition, a relatively large $A_{\rm BG}$ compared with $A_{\rm KT1}$ and $A_{\rm KT2}$ is due to a small sample size.

DFT calculations with generalized gradient approximation (GGA) [16] predicted the presence of two muon sites in the lattice (Fig. 3 and Table 1). The ratio between Δs for the two sites is 6.9(= 2.33/0.377) from the experiment, vs. 2.0(= 0.4860/0.2425) from the calculations. Note that only nuclear magnetic moments were taken into account for the calculations. Since Δ_2 ranges between the two predicted values, the muons at one site, probably at the μ_2 site, clearly *see* a nuclear magnetic field. However, Δ_1(= 2.33×10^6 sec^{-1} $\sim$ 27 Oe) is rather large compared with the predicted values. This implies that the muons at the μ_1 site sense not only a nuclear magnetic field but also randomly distributed localized magnetic moments of Co, which appear below 10 K. The magnitude of such localized moment is estimated as 0.014 $\mu_{\rm B}$. Note that $A_{\rm KT1}/(A_{\rm KT1} + A_{\rm KT2}) = 0.28$, corresponding to that 28 % muons in the $SrCo_2P_2$ sample see the internal magnetic field due to the Co moments. Therefore, such behavior is not induced by magnetic impurities but an intrinsic nature of $SrCo_2P_2$ and is likely to suggest the appearance of short-range correlation below 10 K. This is because ZF- and LF-spectra for the ordered phase is not explained by a static Kubo-Toyabe function [8].

Table 1: Possible muon sites (μ_n) and the field distribution width in $SrCo_2P_2$ and $CaCo_2P_2$ predicted by DFT calculations with GGA and dipole field calculations. The optimized structural parameters (and experimental values [5, 17]) are a = 3.792 (3.760) Å, c = 11.793 (11.602) Å, and z = 0.3511 (0.3525) for $SrCo_2P_2$, and a = 3.843 (3.85) Å, c = 9.603 (9.55) Å, and z = 0.3714 (0.3722) for $CaCo_2P_2$. Here, the atomic positions of Sr/Ca, Co, and P are (0,0,0), (0,1/2,1/4), and (0,0,z), respectively. Δ is calculated based only on nuclear magnetic moments and 1 Oe corresponds to 0.08516×10^6 s^{-1}. E represents the potential energy. There are 4 equivalent positions in the unit cell for the 4e sites, 2 equivalent positions for the 2b sites, and 32 equivalent positions for the 32o sites. One of them for each site is shown in Fig. 3.

compound	site	(x, y, z)	E (eV)	Δ (Oe)	Δ (10^6 s^{-1})
$SrCo_2P_2$	4e (μ1)	(0.0000,0.0000,0.1954)	-13.93	5.707	0.4860
	2b (μ2)	(0.0000,0.0000,0.5000)	-14.10	2.848	0.2425
$CaCo_2P_2$	4e (μ1)	(0.0000,0.0000,0.1991)	-14.10	5.912	0.5035
	32o (μ2)	(0.5099,0.0253,0.0717)	-14.23	4.944	0.4210

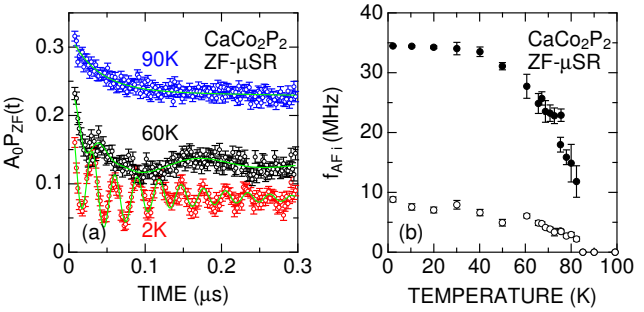

Figure 4: (a) the ZF-μ^+SR spectra for $CaCo_2P_2$ obtained at 2, 60, and 90 K. Each spectrum is shifted upward by 0.05 for clarity of display. (b) the temperature dependence of the muon spin precession frequencies ($f_{\rm AFi}$) in $CaCo_2P_2$. Solid lines in (a) represent the best fit using Eq. (2).

3.2 $CaCo_2P_2$

Neutron diffraction studies [5] revealed that $CaCo_2P_2$ is an antiferromagnetic metal with $T_{\rm N} \sim$ 85 K, below which the Co moments ($\mu_{\rm Co}$) are aligned ferromagnetically in the c-plane, but antiferromagnetically along the c-axis below $T_{\rm N}$, i.e. the A-type AF order with $\boldsymbol{q}$=(0,0,1). The ZF-μ^+SR spectrum for $CaCo_2P_2$ exhibits a clear oscillation due to the formation of static AF order below $T_{\rm N}$. Since there are two oscillatory signals with different muon spin precession frequencies, the ZF spectrum was fitted by

$$A_0\, P_{\rm ZF}(t) = \sum_{i=1}^{2} A_{{\rm AF}i}\, \cos(2\pi f_{{\rm AF}i} t + \phi_i)\, \exp\left(-\lambda_{{\rm AF}i}\right) + A_{\rm tail} \exp(-\left(\lambda_{\rm tail} t\right)^{\gamma}) + A_{\rm BG} G(\Delta_{\rm BG}, t), \quad (2)$$

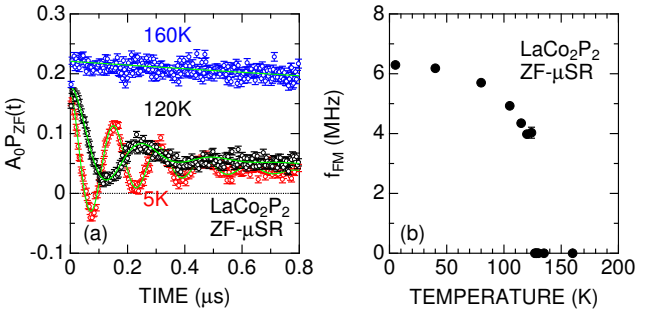

Figure 5: (a) the ZF-μ^+SR spectra for $LaCo_2P_2$ obtained at 5, 120, and 160 K. (b) the temperature dependence of the muon spin precession frequency ($f_{\rm FM}$) in $LaCo_2P_2$. Solid lines in (a) represent the best fit using Eq. (3).

where A_i are the asymmetries and $A_{\rm tail} = \frac{1}{2}\sum A_{{\rm AF}i}$, λ_i are exponential relaxation rates, and $2\pi f_i (\equiv \omega_i)$ are the muon Larmor frequencies of the three signals. G is a static Kubo-Toyabe function [18], $G = \frac{1}{3} + \frac{2}{3}(1-\Delta^2 t^2)\exp(-\frac{1}{2}\Delta^2 t^2)$, and Δ (in this case $\Delta_{\rm BG}$) is proportional to the field distribution width at the muon site. The $A_{\rm tail}$ signal corresponds to the ZF "1/3 tail" due to the field component parallel to the initial muon spin polarization. Finally, the $A_{\rm BG}$ signal corresponds to a static nuclear field component due to a nonmagnetic impurity phase with about 13 vol%, most likely CaP. In fact, $\Delta_{\rm BG} = 0.358(8)\times 10^6$ s^{-1} (implying a distribution of local fields with a width of ~ 4.2 Oe) at 2 K and was almost T independent until $T_{\rm N}$.

Both $f_{\rm AF1}(T)$ and $f_{\rm AF2}(T)$ curves show an order parameter like T dependence and drop to zero at $T_{\rm N}$ [see Fig. 4(b)], indicating the presence of two magnetically different muon sites in the lattice, as predicted by DFT calculations [Fig. 3(b) and Table 1]. If we compare the internal magnetic field estimated by dipole field calculations at the two muon sites with the experimental results, we obtain that $\mu_{\rm Co} = 0.41(1)\ \mu_{\rm B}$ at 2 K, which is roughly comparable to the past neutron work ($0.32\ \mu_{\rm B}$) [5]. Such small $\mu_{\rm Co}$ compared with the effective magnetic moment of Co ($\mu_{\rm eff} \sim 1.7\ \mu_{\rm B}$ [4]) supports an itinerant electron nature of $CaCo_2P_2$.

3.3 $LaCo_2P_2$

$LaCo_2P_2$ is known as a ferromagnetic metal with $T_{\rm C} = 132$ K [19]. Figure 5(a) shows the variation of the ZF-μ^+SR spectrum with temperature. Since the spectrum below $T_{\rm C}$ exhibits a clear oscillation due to the formation of a static magnetic field, the spectrum was fitted by a combination of an exponentially damped cosine oscillation for the static internal magnetic field and an exponentially damped non-oscillatory signal for a "1/3" tail for a powder sample;

$$A_0\, P_{\rm ZF}(t) \quad = \quad A_{\rm FM}\exp(-\lambda_{\rm FM}t)\cos(2\pi f_{\rm FM}t + \phi_{\rm FM}) + A_{\rm tail}\exp(-\lambda_{\rm tail}t), \qquad (3)$$

where A_i are the asymmetries, λ_i are the exponential relaxation rates, $f_{\rm FM}$ is the muon spin precession frequency, and $\phi_{\rm FM}$ is the initial phase.

Figure 5(b) shows the temperature dependence of $f_{\rm FM}$ for $LaCo_2P_2$. The $f_{\rm FM}(T)$ curve exhibits an order parameter-like temperature dependence, as expected. However, for unmagnetized ferromagnetic materials in zero applied field, the internal magnetic field at a muon site

($\boldsymbol{H_\mu}$) is represented by [20, 21, 22];

$$\boldsymbol{H_\mu} = \boldsymbol{H_{dip}} + \boldsymbol{H_L} + \boldsymbol{H_{hf}}, \quad (4)$$

where $\boldsymbol{H_{dip}}$ is the dipolar field, $\boldsymbol{H_L}$ is the Lorentz field, and $\boldsymbol{H_{hf}}$ is the hyperfine field. Furthermore, $\boldsymbol{H_L}$ and $\boldsymbol{H_{hf}}$ are connected to the saturated magnetization ($\boldsymbol{M_s}$) and the local spin density at the muon sites (ρ_{spin}), as follows;

$$\begin{aligned} \boldsymbol{H_L} &= 4\pi/3 \times \boldsymbol{M_s}, \\ \boldsymbol{H_{hf}} &= 8\pi/3 \times \rho_{spin}(\boldsymbol{r_\mu}). \end{aligned} \quad (5)$$

Since $M_s = 0.391$ μ_B/Co along the a-axis at 5 K [19], $\boldsymbol{H_L}$ is calculated as (190, 0, 0) Oe [22].

If we assume that the implanted muons locate at the $\mu 1$ site, as in the case for $SrCo_2P_2$, and that the Co moments align along the a-axis, as proposed by neutron diffraction measurements, then H_{dip}=1884 Oe/μ_B along the a-axis. Since the ordered moment was reported as μ_{ord} = 0.47(5) μ_B, $\boldsymbol{H_{dip}}$=(885, 0, 0) Oe and $\boldsymbol{H_{hf}}$=(-610, 0, 0) Oe. Thus, $\boldsymbol{H_{hf}}$ is found to be almost comparable to $\boldsymbol{H_{dip}}$, as in the case of other ferromagnetic materials [22, 23, 24].

4 Summary

The magnetic phase diagram of the solid solution system between $SrCo_2P_2$ and $CaCo_2P_2$ was studied with μ^+SR using mainly powder samples. The end compound, $SrCo_2P_2$, was found to be an enhanced paramagnetic metal [25] down to 19 mK, although small random localized magnetic moments, which probably suggests the presence of short-range correlation, appear below 10 K. The other end compound, $CaCo_2P_2$, enters into an A-type antiferromagnetic ordered phase below $\sim$ 85 K. The isostructural compound, $LaCo_2P_2$, was found to undergo a magnetic transition below $\sim$ 130 K. Using the past neutron data, the hyperfine field was also estimated.

5 Acknowledgments

We thank the staff of TRIUMF and PSI for help with the μ^+SR experiment. All images involving crystal structure were made with **VESTA** [26]. MM was supported by Marie Skłodowska Curie Action, International Career Grant through the European Union and Swedish Research Council (VR), Grant No. INCA-2014-6426. D.A. acknowledges partial financial support from Romanian UEFISCDI Project No. PN-II-ID-PCE-2011-3-0583 (85/2011). This work was supported by MEXT KAKENHI Grant No. 23108003 and JSPS KAKENHI Grant No. 26286084.

References

[1] M. S. Torikachvili, S. L. Bud'ko, N. Ni, and P. C. Canfield. Pressure Induced Superconductivity in $CaFe_2As_2$ *Phys. Rev. Lett.* 101(5): 057006, Aug 2008.

[2] A. Kreyssig, M. A. Green, Y. Lee, G. D. Samolyuk, P. Zajdel, J. W. Lynn, S. L. Bud'ko, M. S. Torikachvili, N. Ni, S. Nandi, J. B. Leão, S. J. Poulton, D. N. Argyriou, B. N. Harmon, R. J. McQueeney, P. C. Canfield, and A. I. Goldman. Pressure-induced volume-collapsed tetragonal phase of $CaFe_2As_2$ as seen via neutron scattering *Phys. Rev. B* 78(18): 184517, Nov (2008).

[3] M. Rotter, M. Tegel, and D. Johrendt. Superconductivity at 38 K in the Iron Arsenide $(Ba_{1-x}K_x)Fe_2As_2$. *Phys. Rev. Lett.* 101(10): 107006, Sep 2008.

[4] S. Jia, A. J. Williams, P. W. Stephens, and R. J. Cava. Lattice collapse and the magnetic phase diagram of $Sr_{1-x}Ca_xCo_2P_2$. *Phys. Rev. B*, 80(16): 165107, Oct 2009.

[5] M. Reehuis, W. Jeitschko, G. Kotzyba, B. Zimmer, and X. Hu. Antiferromagnetic order in the $ThCr_2Si_2$ type phosphides $CaCo_2P_2$ and $CeCo_2P_2$. *J. Alloys Compounds*, 266(1-2): 54–60, Feb 1998.

[6] Jia, S. Chi, J. W. Lynn, and R. J. Cava. Magnetic and structural properties of $Ca(Fe_{1-x}Co_x)_2P_2$ and $Ca(Ni_{1-x}Co_x)_2P_2$. *Phys. Rev. B*, 81(21): 214446, Jun 2010.

[7] S. Jia, P. Jiramongkolchai, M. R. Suchomel, B. H. Toby, J. G. Checkelsky, N. P. Ong, and R. J. Cava. Ferromagnetic quantum critical point induced by dimer-breaking in $SrCo_2(Ge_{1-x}P_x)_2$. *Nature Phys.*, 81(21): 207–210, Jun 2011.

[8] J. Sugiyama, H. Nozaki, I. Umegaki, M. Harada, Y. Higuchi, K. Miwa, E. J. Ansaldo, J. H. Brewer, M.i Imai, C. Michioka, K. Yoshimura, and M Månsson. Variation of magnetic ground state of $Sr_{1-x}Ca_xCo_2P_2$ determined with μ^+SR. *Phys. Rev. B*, 91(14): 144423, Apr 2015.

[9] G. M. Kalvius, D. R. Noakes, and O. Hartmann. *Handbook on the Physics and Chemistry of Rare Earths*. volume 32, chapter 206, pages 55–451. North-Holland, Amsterdam, 2001.

[10] A. Yaouanc and P. Dalmas de Reotier. *Muon Spin Rotation, Relaxation, and Resonance: Applications to Condensed Matter*. Oxford, Oxford, 2011.

[11] K. Mukai, Y. Ikedo, H. Nozaki, J. Sugiyama, P. L. Russo, K. Nishiyama, D. Andreica, A. Amato, J. H. Brewer, E. J. Ansaldo, K. H. Chow, K. Ariyoshi, and T. Ohzuku. Magnetic phase diagram in layered cobalt dioxide Li_xCoO_2. *Phys. Rev. Lett.* 99(8): 087601, Aug 2007.

[12] J. Sugiyama, K. Mukai, Y. Ikedo, H. Nozaki, P. L. Russo, D. Andreica, A. Amato, K. Ariyoshi, and T. Ohzuku. Static magnetic order on the triangular antiferromagnet Li_xNiO_2 with $x \leq 1$. *Phys. Rev. B* 78(14): 144412, Oct 2008.

[13] J. Sugiyama, Y. Ikedo, T. Goko, E. J. Ansaldo, J. H. Brewer, P. L. Russo, K. H. Chow, and H. Sakurai, Complex magnetic phases in $Ca_{1-x}Na_xV_2O_4$ with $0 \leq x \leq 1$. *Phys. Rev. B* 78(22): 224406, Dec 2008.

[14] M. Imai, C. Michioka, H. Ohta, A. Matsuo, K. Kindo, H. Ueda, and K. Yoshimura. Anomalous itinerant-electron metamagnetic transition in the layered $Sr_{1-x}Ca_xCo_2P_2$ system. *Phys. Rev. B*, 90(1): 014407, Jul 2014.

[15] A. Teruya, A. Nakamura, T. Takeuchi, H. Harima, K. Uchima, M. Hedo, T. Nakama, and Y. Onuki. De Haas-van Alphen effect and Fermi surface properties in nearly ferromagnet $SrCo_2P_2$. *J. Phys. Soc. Jpn.* 83(11): 113702, Oct 2014.

[16] T. Sato, K. Miwa, Y. Nakamori, K. Ohoyama, H.-W. Li, T. Noritake, M. Aoki, S. I. Towata, and S. I. Orimo. Experimental and computational studies on solvent-free rare-earth metal borohydrides $R(BH_4)_3$ (R = Y, Dy, and Gd) *Phys. Rev. B* 77(10): 104114, Mar 2008.

[17] M. Reehuis and W. Jeitschko, Structure and magnetic properties of the phosphides $CaCo_2P_2$ and LnT_2P_2 with $ThCr_2Si_2$ structure and LnTP with PbFCl structure (ln =lanthanoids, T = Fe, Co, Ni). *J. Phys. Chem. Solids* 51(8): 961–968, 1990.

[18] R. S. Hayano, Y. J. Uemura, J. Imazato, N. Nishida, T. Yamazaki, and R. Kubo. Zero-and low-field spin relaxation studied by positive muons. *Phys. Rev. B*, 20(3): 850-859, Aug 1979.

[19] M. Reehuis and C. Ritter, R. Ballou, and W. Jeitschko. Ferromagnetism in the $ThCr_2Si_2$ type phosphide $LaCo_2P_2$. *Journal of Magnetism and Magnetic Materials* 138(1-2): 85-93, Nov 1994.

[20] A. Schenck, *Muon spin rotation spectroscopy, Principles and applications in solid state physics*. pages 162–181. Adam Hilger, Bristol, 1985.

[21] S. Barth, E. Albert, G. Heiduk, A. Moslang, A. Weidinger, E. Recknagel, and K. H. J. Buschow. Local magnetic fields in ferromagnetic intermetallic compounds of cubic Laves-phase type. *Phys. Rev. B*, 33(1): 430–436, Jan 1986, and references cited therein.

[22] J. Sugiyama, H. Nozaki, M. Månsson, K. Prša, D. Andreica, A. Amato, M. Isobe, and Y. Ueda. μ^+SR study on ferromagnetic hollandite $K_2Cr_8O_{16}$ and $Rb_2Cr_8O_{16}$. *Phys. Rev. B*, 85(21): 214407,

Jun 2014.

[23] Ch. Niedermayer, A. Golnik, E. Recknagel, A. Weidinger, A. J. Yaouanc, Ph. L'heritier, D. Fruchart, J. I. Budnick, and K. H. J. Buschow. Positive muon spectroscopy of $R_2Fe_{14}B$. *Hyperfine Interactions*, 64(1–4): 405–414, Feb 1991.

[24] S. J. Blundell, T. Lancaster, F. L. Pratt, P. J. Baker, W. Hayes, J.-P. Ansermet, and A. Comment. Phase transition in the localized ferromagnet EuO probed by μSR. *Phys. Rev. B*, 81(9): 092407, Mar 2010.

[25] E. Mörsen, B. D. Mosel, Wüller-Warmuth, M. Reehuis, and W. Jeitschko. Mössbauer and magnetic susceptibility investigations of strontium, lanthanum and europium transition metal phosphides with $ThCr_2Si_2$ type structure. *J. Phys. Chem. Solids*, 49(7): 785–795, 1988.

[26] K. Momma and F. Izumi. VESTA: a three-dimensional visualization system for electronic and structural analysis. *J. Appl. Cryst.*, 41(3): 653–658, Jun 2008.